DOI: 10.1534/genetics.107.080515

The *Caenorhabditis elegans ing-3* Gene Regulates Ionizing Radiation-Induced Germ-Cell Apoptosis in a p53-Associated Pathway

Jingjing Luo,*,† Sitar Shah,*,† Karl Riabowol*,† and Paul E. Mains†,‡,§,1

**Department of Oncology,* †*Department of Biochemistry and Molecular Biology,* ‡*Department of Medical Genetics and* §*Genes and Development Research Group, University of Calgary, Calgary, Alberta T2N 4N1, Canada*

Manuscript received August 15, 2007
Accepted for publication November 13, 2008

ABSTRACT

The *in*hibitor of *g*rowth (ING) family of type II tumor suppressors are encoded by five genes in mammals and by three genes in *Caenorhabditis elegans*. All ING proteins contain a highly conserved plant homeodomain (PHD) zinc finger. ING proteins are activated by stresses, including ionizing radiation, leading to the activation of p53. ING proteins in mammals and yeast have recently been shown to read the histone code in a methylation-sensitive manner to regulate gene expression. Here we identify and characterize *ing-3*, the *C. elegans* gene with the highest sequence identity to the human *ING3* gene. ING-3 colocalizes with chromatin in embryos, the germline, and somatic cells. The *ing-3* gene is part of an operon but is also transcribed from its own promoter. Both *ing-3(RNAi)* and *ing-3* mutant strains demonstrate that the gene likely functions in concert with the *C. elegans* p53 homolog, *cep-1*, to induce germ-cell apoptosis in response to ionizing radiation. Somatically, the *ing-3* mutant has a weak kinker uncoordinated (kinker Unc) phenotype, indicating a possible neuronal function.

THE founding member of the *in*hibitor of *g*rowth (ING) family was first identified as a growth inhibitor and type II tumor suppressor expressed in normal, but not in cancerous, cells (Garkavtsev *et al.* 1996). ING proteins have since been implicated in diverse biological processes, including angiogenesis, apoptosis, DNA repair, cell cycle regulation, oncogenesis, regulation of gene expression, and stress signaling (reviewed in Russell *et al.* 2006). ING proteins bind a wide range of cellular proteins, including proliferating cell nuclear antigen (Scott *et al.* 2001) as well as histone acetyltransferase (HAT) and histone deacetylase (HDAC) complexes (reviewed in Russell *et al.* 2006). In particular, ING proteins interact genetically and physically with the p53 tumor suppressor during stress responses and apoptosis (Garkavtsev *et al.* 1998; Nourani *et al.* 2003).

More than 60 *ING* genes have been identified in a broad range of species on the basis of sequence similarity (He *et al.* 2005), and all contain a highly conserved plant homeodomain (PHD), a Cys4-His-Cys3 form of zinc finger (Bienz 2006) associated with chromatin remodeling. The PHD region of ING proteins interacts directly with histone H3, and a subset of ING proteins does this in a methylation-sensitive manner (Martin *et al.* 2006; Pena *et al.* 2006; Shi *et al.* 2006). These properties, combined with observations that the ING proteins serve as receptors and transducers of stress-activated phosphoinositides (Gozani *et al.* 2003; Kaadige and Ayer 2006), suggest that ING proteins link key pathways involved with regulating chromatin structure, histone methylation, and histone acetylation.

The five mammalian *ING* genes (Nagashima *et al.* 2001, 2003; Feng *et al.* 2002) fall into three subgroups (He *et al.* 2005). Although the mammalian ING family subgroups (ING1–5) share structural (He *et al.* 2005) and functional features (Doyon *et al.* 2006) and appear to play roles in interpreting the epigenetic histone code (Martin *et al.* 2006; Palacios *et al.* 2006; Pena *et al.* 2006; Shi *et al.* 2006), little is known about their function in intact organisms. In *Saccharomyces cerevisiae*, deletion of any of the three *ing* homologous genes, *yng1*, *yng2*, and *yng3*, results in pleiotropic phenotypes (Loewith *et al.* 2000). For example, most mutants and mutant combinations germinate and grow, but *yng2* knockout cells grow slowly and are enlarged and multibudded, with buds frequently devoid of DNA. Triple *yng* mutants are viable but show severe growth inhibition and more exaggerated morphological and multibudded phenotypes. Mutants in each gene are hypersensitive to heat shock. Deletion of *yng2* alone results in sensitivity to UV irradiation but not to γ-irradiation or treatment with alkylating agents (Loewith *et al.* 2000). The *yng* stress-associated functions may be related to the observation that mammalian *ING1* and *ING2* both induce hsp70 heat-shock protein (Feng *et al.* 2006).

As with humans, mice harbor five *ING* genes. The only reported knockout, *ING1*, is viable, but animals have an

[1]*Corresponding author:* Department of Biochemistry and Molecular Biology, University of Calgary, 3330 Hospital Dr. NW, Calgary, AB T2N 4N1, Canada. E-mail: mains@ucalgary.ca

increased incidence of B-cell lymphomas and sensitivity to γ-radiation (Kichina *et al.* 2006; Coles *et al.* 2007), consistent with *ING1* being a type II tumor suppressor. However, although previous cell culture results clearly indicate that *ING* proteins interact both physically and genetically with p53 (Garkavtsev *et al.* 1998; Shinoura *et al.* 1999; Shiseki *et al.* 2003; reviewed in Soliman and Riabowol 2007), neither *ING1* deletion mice nor their derived cell lines demonstrated that *ING1* function depends upon p53 or that p53 function is perturbed in *ING1* knockouts (Coles *et al.* 2007).

To explore the developmental role(s) of ING proteins, and particularly a relationship to p53, we studied the function of *Caenorhabditis elegans ing-3*, the *ING* gene most similar in worms and humans. We found that ING-3 is widely expressed and localizes to chromatin. Unlike yeast (Loewith *et al.* 2000), no changes were seen in response to UV damage after *ing-3(RNAi)*. However, similar to what is seen in mice, reduction or loss of *C. elegans* ING-3 alters the response to γ-radiation, as indicated by decreased germline apoptosis, which in turn leads to increased embryonic lethality. Unlike the mouse *ING1* mutant, we find that *ing-3* does operate in concert the *C. elegans* p53 homolog *cep-1* to mediate apoptosis. The phenotypes that we report are the first to demonstrate a role for an ING protein in the germline or embryo.

MATERIALS AND METHODS

Strains: Animals were cultured at 20° as described (Brenner 1974). Wild type was Bristol N2, and mutant strains include *cep-1(gk138)*, *rrf-3(pk1426)*, and *mcd-1(tm2169)* (http://www.wormbase.org; WS170 data freeze). *ing-3(tm2530)* and *ing-3(ttTi5439)* were generously provided by the Japanese National Bioresource Project for the Nematode (Gengyo-Ando and Mitani 2000) and the *Mos* transposon insertion from the NEMAGENETAG Consortium (Granger *et al.* 2004), respectively. *ing-3* mutants were outcrossed three times.

Identification of homologs: Homologs of the *ing-3* gene were identified in *Caenorhabditis briggsae*, Drosophila, Xenopus, mice, and humans with the BLAST program at the National Center for Biotechnology Information (NCBI) (http://www.ncbi.nlm.nih.gov/BLAST). The multiple sequence alignments of ING3 were created with the CLUSTAL W program at the European Bioinformatics Institute (http://www.ebi.ac.uk/clustalw/).

Nomarski differential interference contrast microscopy: Worms were observed on 3% agarose pads and anesthetized with 10 mm levamisole (Shaham 2006). Worms, both by Nomarski and immunofluorescence, were visualized using an Axioscope microscope (Zeiss) and images were processed using AxioVision (Zeiss) and Photoshop 7.0 (Adobe) software.

Antibody production and Western blots: Mouse polyclonal antibodies against *C. elegans* ING-3 were generated at the Southern Alberta Cancer Research Institute Antibody Services against the keyhole limpet hemocyanin-conjugated peptide CEMEADNSGVTEMIE [amino acid residues 108–122, a highly conserved hydrophilic motif within the lamin interacting domain (LID)]. Gravid adults were used in Western blots, which were performed as described (Feng *et al.* 2006) using a 2000-fold dilution of anti-ING-3 antiserum incubated overnight at 4°.

Immunostaining: Adult hermaphrodite gonads were fixed in 100% methanol as described (Hansen *et al.* 2004). Dissected gonads were incubated overnight at 4° with mouse anti-ING-3 antiserum, diluted 1:100. Goat anti-mouse IgG-Texas Red (Sigma) was used at 1:100 dilution as the secondary antibody. DAPI (4′,6-diamidino-2-phenylindole) was added at 0.5 μg/ml to stain DNA.

Embryos were fixed and permeablized by freeze-cracking as described (Miller and Shakes 1995). Staining was at the same antibody concentrations as for the gonads, but incubations with primary and secondary antibodies were for 45 min and 1 hr, respectively.

Plasmid construction: To determine the structure of *ing-3* transcripts, a cDNA pool of mixed-stage worms was subjected to PCR amplification. A pair of specific primers (F1 and R1, listed below) flanking the start and stop codons amplified the coding region. A poly(T) primer and nested gene-specific primers (F2 and F3) amplified the 3′-end while the splice leaders SL1 and SL2 and the nested gene-specific primers (R2 and R3) amplified the 5′-end. PCR products were gel purified and then sequenced by the University of Calgary DNA lab.

The genomic sequences of the operon promoter (600 bp) and the *ing-3* internal promoter (880 bp) were obtained by PCR and subcloned into the promoterless GFP-LacZ reporter vector pPD96.04 (gift from Andrew Fire, Stanford University) to create the transcriptional *ing-3* promoter-*gfp-LacZ* fusions.

The following primers were used: F1, 5′-CATTGCAT GCCTCTTCCTCGATGATTTTTT-3′; R1, 5′-CAGAAGCTTT TAGACTTCTCCCTCTTCGG-3′; SL1, 5′-GGTTTAATTACCC AAGTTTGAG-3′; SL2, 5′-GGTTTTAACCCAGTTACTCAAG-3′; R2, 5′-ATTTGCGTTGAGCTAGCACG-3′; R3, 5′-CGGTCACTC CTGAATTGTCG-3′; F2, 5′-AGAAGAGCTATGGAGATATG-3′; and F3, 5′-ATCGGAGG ATGAGGAGGATG-3′.

Transgenesis: Transgenic strains were created by injecting 50 ng/ml of the *promoter-gfp-LacZ* plasmid DNA with 50 ng/ml of pRF4 [*rol-6(su1006dm)*] into the gonad of young adult hermaphrodites (Mello *et al.* 1991). The presence of the constructs was confirmed in Roller offspring by PCR. All six transgenic lines made for each promoter plasmid showed the same GFP and LacZ expression patterns. For β-Gal staining, worms in M9 buffer were dried on slides for 10 min, fixed, and permeablized with acetone for 30 min and then incubated overnight with X-Gal (Zdinak *et al.* 1997).

RNA interference: RNA interference (RNAi) for *ing-3* was performed using standard bacterial feeding and injection methods (Timmons *et al.* 2001). A 463-bp fragment of *ing-3* (see Figure 1C) was cloned into the RNAi feeding vector L4440, transformed into *Escherichia coli* HT115, and induced with isopropyl-β-d-thiogalactopyranoside. Wild-type worms fed on *E. coli* HT115 containing the vector L4440 were used as controls. The following primers were used: ING3F (5′-ACAGTCTCCATTCCAAGTGCTCT-3′) and ING3R (5′-AAC TCGGTCCTTCCTCATCATCA-3′).

For injection, double-strand RNA (dsRNA) was generated by *in vitro* transcription with a MEGAscript purification kit (Ambion) and dsRNA *gfp* was used as a control. Sense and antisense RNAs were transcribed separately and mixed together in equimolar amounts. dsRNA was injected at 1 μg/μl into the gonads of young adult hermaphrodites, worms were transferred to new plates 12 hr later, and phenotypes were scored in the next 24-hr brood. *ing-3* feeding and injection gave similar results.

Ionizing radiation-induced embryonic lethality: One-day post-L4 gravid adults treated with RNAi were exposed to different doses of γ-radiation using a ^{137}Cs source. Following irradiation, worms were immediately transferred to new plates, and eggs laid during the first 0–8 hr (irradiated at diakinesis through embryogenesis) or 8–22 hr (irradiated at pachytene;

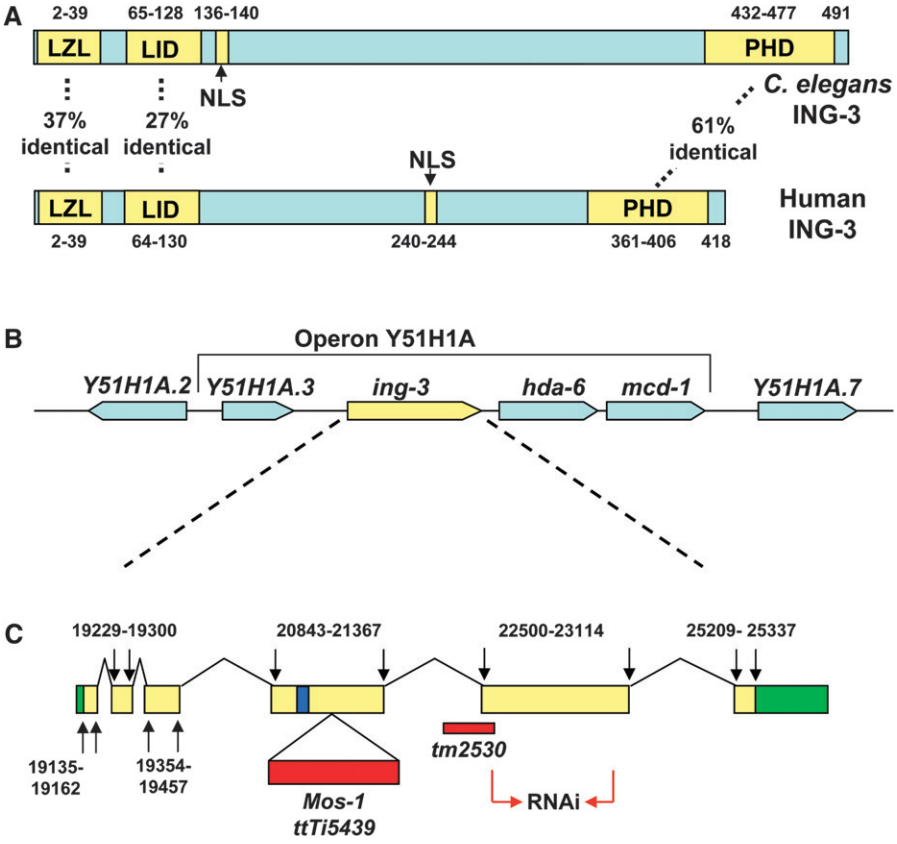

FIGURE 1.—*ing-3* protein and gene structure. (A) Diagram of the predicted ING-3 protein, indicating the PHD, leucine zipper-like domain (LZL), the NLS, and the LID. The corresponding regions and amino acid similarities with human ING-3 are shown. (B) The *ing-3* gene is the second gene in a predicted operon that includes mitochondrial dehydrogenase (*Y51H1A.3*) and histone deacetylase *hda-6* and *mcd-1*. (C) The six exons of the *ing-3* gene are indicated by yellow boxes while green boxes represent the 5′ and 3′ untranslated regions. The relative exon positions on cosmid Y51H1A are indicated. The position of the alleles *ttTi5439* and *tm2530* are shown in red, and the blue box indicates the region used to raise the antisera. The region used to generate dsRNA for RNAi is marked with red arrows.

TAKANAMI *et al.* 2000) were scored for hatching 24 hr after removal of the parents.

Ionizing radiation-induced germ-cell death: L4-stage larvae were treated with 120 Gy of γ-radiation. The number of apoptotic germ cells per gonad arm was counted 24 hr later using Nomarski optics (GUMIENNY *et al.* 1999; GARTNER *et al.* 2000) or acridine orange (AO; GARTNER *et al.* 2004; LETTRE *et al.* 2004). Worms were incubated with 500 μl of 100 mM AO on plates for 1 hr, transferred to new plates in the dark, and 1 hr later were mounted on slides and observed by fluorescence microscopy.

Statistical analyses: The mean number of apoptotic germ cells per gonad and mean embryonic death rate ± standard deviation (SD) are presented. Hypotheses were tested with the two-sided Student's *t*-test.

RESULTS

***C. elegans* has three ING genes:** To identify genes with the highest similarity to human *ING* genes, multiple searches were conducted using the NCBI BLAST program. Three genes, *T06A10.4*, *Y51H1A.4*, and *C11G6.3*, encode ING-related proteins, corresponding to human *ING1–2*, *ING3*, and *ING4–5* subgroups, respectively. As shown in supplemental Table 1, ING3 and Y51H1A.4 had the most significant reciprocal scores in BLAST searches (the human-to-worm score was 1.9×10^{-33}). However, in phylograms drawn by different methods (HE *et al.* 2005), there is not a consistent correspondence between these *C. elegans* genes and the three vertebrate ING subgroups. Using parsimony analysis, *Y51H1A.4* and *C11G6.3* group with ING3, with *Y51H1A.4* being closer, while neighbor-joining analysis suggests that the three worm genes form an outgroup from the vertebrate genes. We chose to focus on the most similar of the worm genes, *Y51H1A.4*, which we designated *ing-3* because this gene and human *ING3* have the highest reciprocal BLAST scores.

Comparison of the primary amino acid sequence of the ING3 proteins from different organisms showed that several regions appeared well conserved (Figure 1A and supplemental Figure 1), including the PHD domain, the leucine zipper-like domain (LZL), the nuclear localization sequence (NLS, although it is in different locations in human and worm proteins), and the lamin interacting domain (LID, SOLIMAN and RIABOWOL 2007; HAN *et al.* 2008).

The *ing-3* gene is expressed in a broad range of tissues: The *C. elegans ing-3* gene is the second gene in a predicted operon that includes mitochondrial dehydrogenase (*Y51H1A.3*), histone deacetylase *hda-6*, and the mediator of the cell death gene *mcd-1* (Figure 1B). As confirmed by RT–PCR, *ing-3* is encoded by six exons (Figure 1C). In *C. elegans*, most mRNAs are *trans*-spliced to one of two 22-nucleotide spliced leaders, SL1 or SL2 (BLUMENTHAL and STEWARD 1997). SL2 is spliced onto the downstream genes in operons, whereas SL1 is used by the first gene in operons and for most non-operon genes. Some downstream genes in operons are also transcribed from both the operon promoter and an internal promoter, in which case the transcripts can be

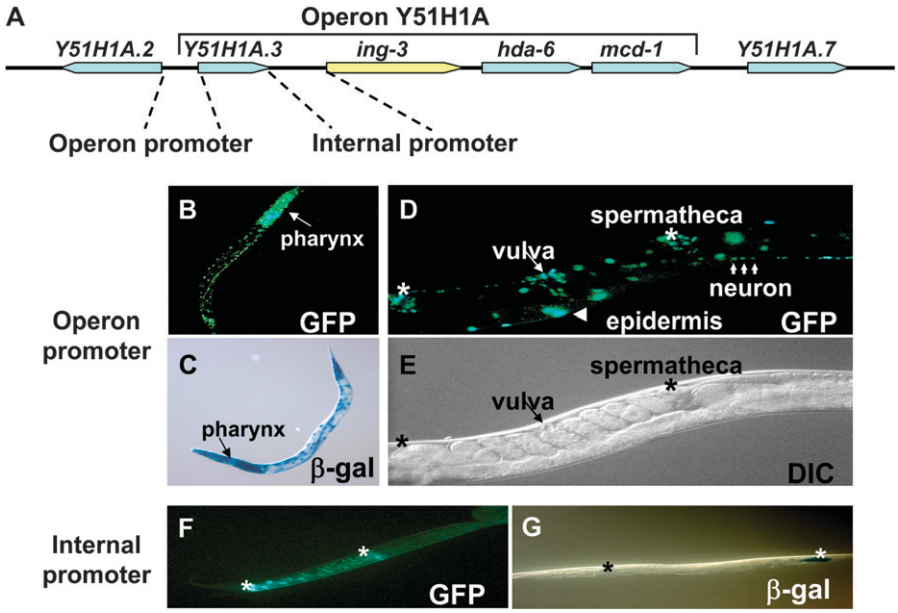

FIGURE 2.—Reporters driven by the operon or internal promoter give different expression patterns. (A) The 5′ genomic sequence (600 bp) of the first gene of this operon (*Y51H1A.3*) was used as the "operon promoter," while the 880 bp between *ing-3* and *Y51H1A.3* was used as the "internal promoter." (B) GFP and (C) LacZ indicate that the operon promoter was widely expressed in L1 larva, especially in the pharynx. (D) The operon promoter showed GFP expression in the adult vulva, spermatheca (asterisks), neurons, and epidermal cells, among others. (E) Differential interference contrast image corresponding to D. The internal promoter expressed GFP (F) and LacZ (G) in the L1 intestine, the limits of which are indicated by asterisks. The signal between the asterisks in F represents gut auto-fluorescence. Note higher expression in the anterior intestinal cells.

spliced to either SL1 or SL2 (BLUMENTHAL and STEWARD 1997). Our RT–PCR analysis indicates that *ing-3* transcripts are spliced to both SL1and SL2 (data not shown).

To determine promoter activity of the regions immediately upstream of the operon and upstream of *ing-3* itself, 600 bp of the 5′ genomic sequence of the first gene in the operon (the "operon promoter") and the 880 bp between *ing-3* and the immediate upstream gene (the "internal promoter") were separately inserted into a *GFP-LacZ* reporter and used to generate transgenic lines (Figure 2A). Expression of the *operon promoter::gfp-LacZ* was first detected during embryogenesis at gastrulation and persisted through adulthood (data not shown). As shown in Figure 2, B–E, GFP and LacZ expression included pharynx, vulva, spermatheca, neurons, and epidermal cells, but not the intestine. In contrast, the expression of the *internal promoter::gfp-LacZ* reporter was first detected at the comma stage, which is later in development than when the *operon promoter::gfp-LacZ* is first detected. Unlike the operon promoter, the internal promoter drives expression in the anterior and posterior intestine cells (Figure 2, F and G), where it persists through adulthood.

ING-3 immunolocalization: Since *C. elegans* transgenes are frequently silenced in the germline (KELLY and FIRE 1998), we produced polyclonal antibodies against a unique and highly conserved hydrophilic region within the LID region of ING-3 (Figure 1A; supplemental Figure 1). Western blots were used to test the specificity of the ING-3 antibody. As shown in Figure 3A, the antibody recognizes only a single band in *ing-3(+)* worms. *ing-3(tm2530)* has a partial deletion in the fourth intron and the fifth exon (Figure 1C) and would potentially encode a truncated product of 28 kDa. In *ing-3(ttTi5439)* worms, the gene is interrupted by a Mos-1 insertion in the fourth exon and would result in a predicted product of 17 kDa. Our mouse polyclonal antibodies recognize a motif encoded before both mutations and so potentially detect these mutant proteins. However, Western blots showed that the wild-type 45-kDa band was missing in both strains and no smaller bands appeared (Figure 3A), suggesting that mutant proteins (or mRNA) are degraded. Thus, these alleles likely represent strong losses of function if not nulls.

We next examined ING-3 localization patterns, particularly in adult germlines and embryos. Figure 3B shows that ING-3 was present in the newly fertilized embryo, where it colocalized with DNA. Similar localization of ING-3 and DAPI continued throughout the embryonic cell cycle, including during mitosis (Figure 3B). This suggests that ING-3 is tightly bound to chromatin at all stages of the cell cycle and so differs from mammalian ING1, which is found throughout the cell during mitosis (HAN *et al.* 2008). ING-3 was also present in the gonad (Figure 3C). Staining was weak in the mitotic proliferating germ cells (region I) but was stronger in the transition zone (region II) and the following early pachytene stages (region III). It decreased by late pachytene and diplotene (region IV). As shown in the higher magnification of gonadal cells, nuclear ING-3 staining, although sometimes uneven, overlapped extensively with DNA. Nuclear staining was absent when antisera were preincubated with the immunizing peptide as well as in the deletion allele *ing-3(tm2530)*, demonstrating antibody specificity. However, nonspecific background staining persisted between cells (this is an unlikely cross-reaction with the other worm ING proteins since they share at most 3/5 consecutive identical amino acids with the immunizing peptide). ING-3 was also expressed in somatic cells where it again overlapped with DAPI, and strong staining was seen for some cells in

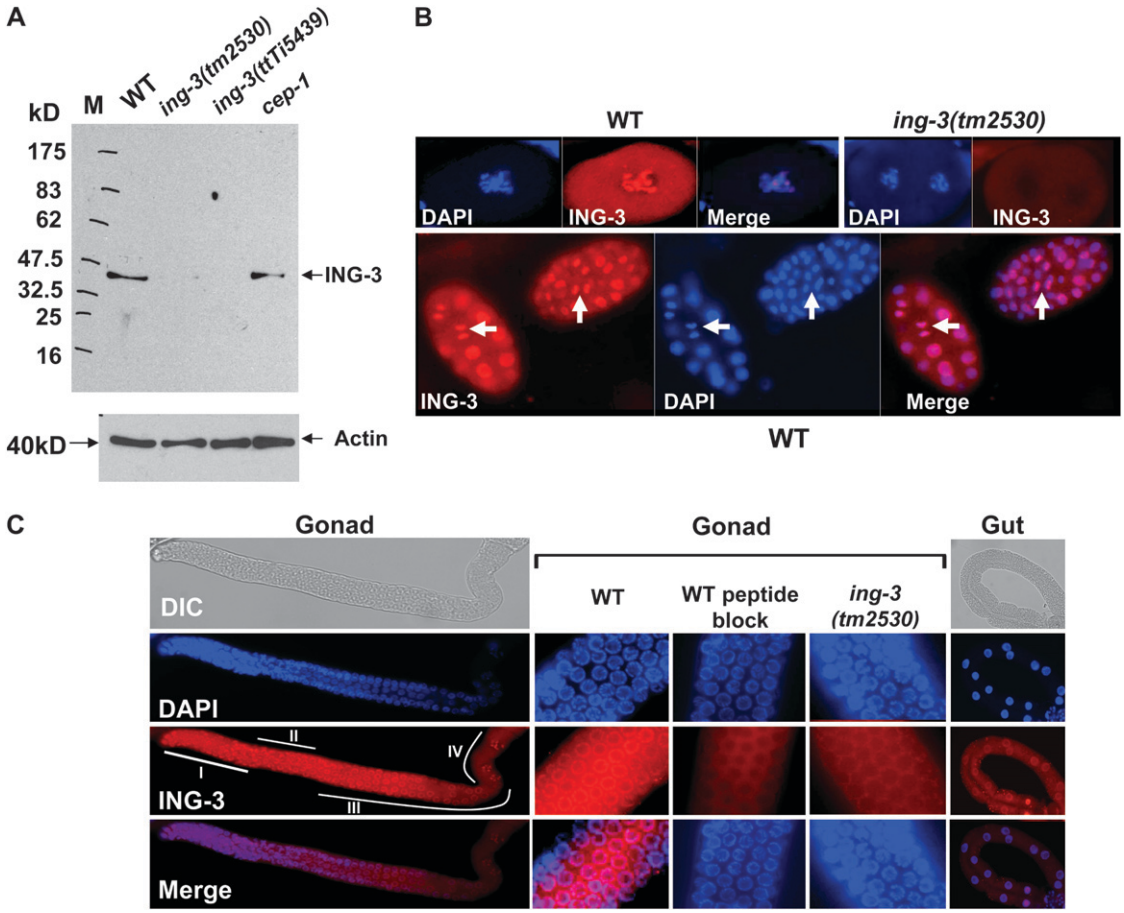

FIGURE 3.—Immunolocalization of ING-3. (A) Mouse polyclonal anti-ING-3 recognized endogenous ING-3 as a single 45-kDa band on Western blots of wild-type gravid hermaphrodites. This band was absent in the two *ing-3* mutants but was present in *cep-1* lysates. Actin was used as the loading control. (B) ING-3 colocalized with chromatin in the newly fertilized embryo (top left) but is absent from *ing-3(tm2530)* (top right). ING-3 was also found on chromatin at mitosis in developing embryos (arrows, bottom row). (C) Immunostaining of dissected wild-type adult gonads (left-most column) shows that ING-3 overlapped DAPI. Lower levels were present in the mitotic region (I) compared to the transition zone (II). High ING-3 persisted into the early pachytene region (III), but then decreased as cells proceeded through meiosis. Low levels, mainly on chromosomes, were seen at diplotene (IV). Higher magnification of the early pachytene section of the gonad (columns 2–4) showed extensive overlap between ING-3 and DAPI. The nuclear signal disappeared when antisera was preincubated with the immunizing peptide (peptide block) or in *ing-3(tm2530)*. Thus the low level of ING-3 staining between cells likely represents background. The right-most column shows the staining pattern for ING-3 in the anterior nuclei of a dissected gut.

the anterior gut (Figure 3C), consistent with results obtained with internal promoter–reporter constructs (Figure 2, F and G).

Depletion of *ing-3* inhibits ionizing radiation-induced germ-cell apoptosis: Since we were particularly interested in the functional relationship between *ing-3* and *cep-1*/p53, we investigated the role of *ing-3* in germline apoptosis, for which *cep-1* has a well-documented phenotype (DERRY *et al.* 2001; SCHUMACHER *et al.* 2001; HOFMANN *et al.* 2002). In mammals, ING proteins also play roles in apoptosis (HELBING *et al.* 1997; NAGASHIMA *et al.* 2003; WANG and LI 2006). We found strong suppression of programmed cell death following ionizing radiation (IR) from γ-rays upon *ing-3* depletion. Twenty-four hours after exposure to 120 Gy of IR, wild type showed a large number of pachytene germ cells undergoing programmed cell death, but many fewer dying cells were present in irradiated *ing-3(RNAi)* animals (Figure 4A). Although the basal level of germline apoptosis was unchanged from wild type in unirradiated *ing-3(RNAi)* animals, the average number of germ-cell corpses was half that of wild type following radiation (Table 1; $P < 0.001$). The *Mos* insertion allele *ing-3(ttTi5439)* was similar to RNAi, while the internal deletion allele *ing-3(tm2530)* had a slightly stronger phenotype (the phenotypes are due to *ing-3* rather than to unknown linked mutations since they are present in two independent alleles). RNAi alone results in a strong loss of function and RNAi treatment did not alter the phenotype of *tm2530*, indicating that *tm2530* is null. Decreased levels of IR-induced apoptosis when *ing-3* was depleted could represent a delay rather than a block to cell death. However, the time course in Figure 4B indicates that this was not the case.

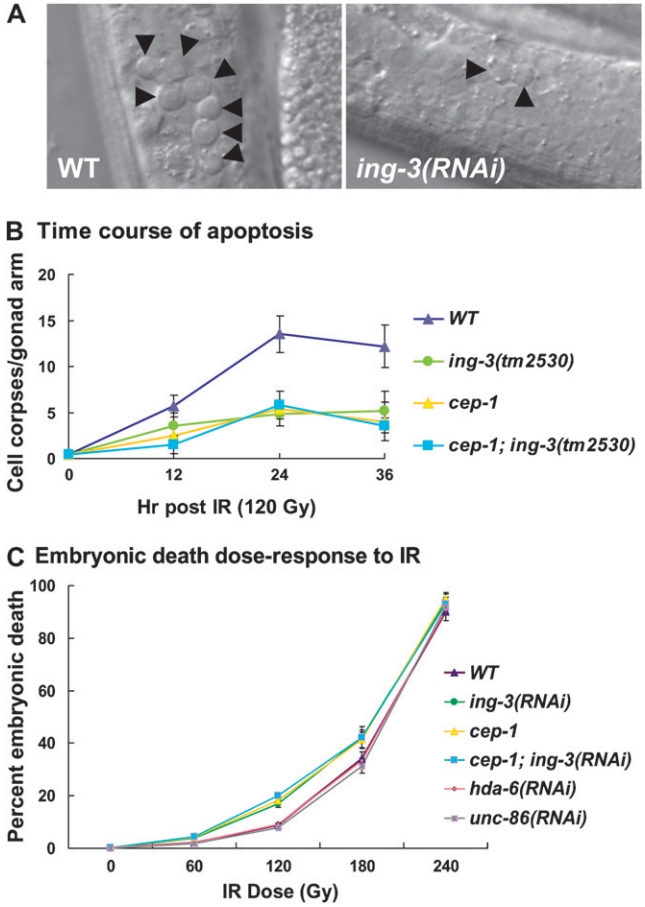

FIGURE 4.—Germ-cell apoptosis and embryonic death following IR. (A) L4 stage larvae were exposed to 120 Gy of IR and the number of apoptotic germ cells (arrowheads) was scored 24 hr later. Animals treated with *ing-3(RNAi)* showed a significantly reduced number of apoptotic germ cells. (B) Time course of accumulation of cell corpses following 120 Gy of IR. Similar to wild type and *cep-1*, apoptosis plateaus by 24 hr in *ing-3* and *ing-3; cep-1*, indicating that *ing-3* is blocking rather than delaying cell death. (C) Dose-response curve of wild type and mutants *vs.* embryonic inviability of the 8- to 22-hr brood following the indicated levels of IR. Error bars represent 1 standard deviation in B and C.

DNA-damaged germ cells that survive due to loss of *ing-3* should give rise to inviable zygotes. The 0- to 8-hr brood after IR corresponds to post-pachytene fertilized embryos or germ cells at the time of exposure. These cells are not sensitive to DNA-damage-induced apoptosis (GARTNER *et al.* 2000; TAKANAMI *et al.* 2000), and therefore apoptosis cannot prevent cells damaged during this time from giving rise to inviable zygotes. Hence, as expected, no change was seen in the viability of wild-type *vs. ing-3(RNAi)* embryos laid 0–8 hr after IR exposure (data not shown). In contrast, *ing-3(RNAi)* nearly doubled the level of embryonic inviability in the 8- to 22-hr brood compared to wild type (Table 2; $P < 0.001$; all data reported below are for this time window). In contrast to IR, we did not find differences in the sensitivity of wild type and *ing-3(RNAi)* to UV (data not shown). As we found for the prevention of germline apoptosis, the *Mos* insertion allele *ttTi5439* was similar to RNAi in increasing embryonic death, while the internal deletion allele *tm2530* showed a stronger, likely null phenotype, since its phenotype was not altered by RNAi (Table 2). We generated an IR dose-response curve for embryonic lethality and found that *ing-3(RNAi)* differed from wild type at both 120 and 180 Gy, with the maximum fold difference (twofold) occurring at 120 Gy (Figure 4C). The RNAi effects were specific as feeding of control *unc-86* dsRNA did not affect embryonic viability (Table 2, Figure 4C).

ing-3 is in the same operon as *hda-6* histone deacetylase (Figure 1B). This is intriguing because mammalian and yeast ING proteins are found in chromatin acetylation and deacetylation complexes (LOEWITH *et al.* 2000; VIEYRA *et al.* 2002b; DOYON *et al.* 2006), and functionally related genes are sometimes found in the same *C.*

TABLE 1

Effects of *ing-3* on germ-cell apoptosis 24 hr after exposure to 120 Gy of IR

Genotype	Germ-cell corpses/gonad arm (±SD)	*N* (gonad arms)
Wild type (no radiation)	3.0 (±1.4)	40
Wild type	13.5 (±2.0)	40
ing-3(RNAi) (no radiation)	2.8 (±1.3)	40
ing-3(RNAi)	6.3 (±1.5)	40
ing-3(ttTi5439)	6.7 (±1.8)	45
ing-3(tm2530)	4.8 (±1.2)	40
ing-3(tm2530; RNAi)	4.9 (±1.4)	30
cep-1(null)	5.4 (±0.8)	30
ing-3(RNAi); cep-1(null)	5.9 (±1.2)	40
ing-3(tm2530); cep-1(null)	5.8 (±1.5)	30

TABLE 2

Unhatched embryos among the brood laid 8–22 hr following exposure of adult hermaphrodites to 120 Gy of IR

Genotype	% embryonic death (±SD)	*N*
Wild type (no radiation)	0.4 (±0.3)	1753
Wild type	9.4 (±0.6)	3078
ing-3(RNAi) (no radiation)	0.2 (±0.1)	1524
ing-3(RNAi)	16.8 (±1.3)	4266
ing-3(ttTi5439)	18.9 (±2.1)	3340
ing-3(tm2530)	22.7 (±2.5)	3431
ing-3(tm2530; RNAi)	23.3 (±4.3)	3125
unc-86(RNAi)	7.9 (±0.8)	2283
hda-6(RNAi)	9.6 (±0.7)	2372
mcd-1(tm2169)	10.2 (±0.9)	2275
cep-1 (no radiation)	0.5 (±0.4)	1602
cep-1	18.2 (±1.9)	3789
ing-3(RNAi); cep-1	20.0 (±1.7)	3672
ing-3(tm2530); cep-1	21.8 (±2.9)	2120

elegans operons (Clark *et al.* 1994; Huang *et al.* 1994; Treinin *et al.* 1998). However, Figure 4C and Table 2 indicate that *hda-6(RNAi)* did not influence embryonic viability following IR (with the caveat that the RNAi is sometimes not effective). Similarly, another member of the operon, *mcd-1*, whose gene product promotes somatic apoptosis (Reddien *et al.* 2007), had no effect in our assay (Table 2; the allele used is predicted to truncate the protein in the second exon, prior to the zinc finger).

***ing-3* acts in the same pathway as *cep-1*/p53:** To determine if *ing-3* acts in concert with p53, we examined genetic interactions between *ing-3* and *cep-1*/p53. Compared to wild type, a *cep-1* deletion allele decreased the number of IR-induced germ-cell corpses and decreased embryonic viability (Tables 1 and 2) to a similar extent as the loss of *ing-3* did [unlike previous reports (Schumacher *et al.* 2001; Quevedo *et al.* 2007), we found that the irradiated *cep-1* levels were slightly above unirradiated controls]. The dose response of embryonic inviability to IR was also similar in *ing-3(RNAi)* and *cep-1* (Figure 4C). If the two mutations act in independent, parallel pathways (and at least one mutation is a null), then the double mutant would show additive effects. However, if the genes act in the same or in convergent pathways, as reported for mammalian ING1 and p53 in some studies (Garkavtsev *et al.* 1998) but not in others (Coles *et al.* 2007), then the double mutant should resemble the individual single mutants. As shown in Table 1, the behavior of *ing-3(RNAi); cep-1* or *ing-3(tm2830); cep-1* indicates that the genes act together since the amount of apoptosis in the double mutants did not decrease below that in the single mutants and remained substantially higher than the basal level of apoptosis in unirradiated wild type ($P < 0.001$). Likewise, the level of embryonic lethality in *ing-3(RNAi); cep-1* or *ing-3(tm2830); cep-1* was similar to *cep-1* alone (Table 2, Figure 4C). In addition, loss of *cep-1* did not affect the level of ING-3 expression (Figure 3A), consistent with reports in other species that expression of ING proteins is independent of p53 (Cheung *et al.* 2000; Coles *et al.* 2007). We observed no changes to the intracellular localization of ING-3 following IR (data not shown).

Since loss of *ing-3* function results in a hyposensitive DNA-damage-induced apoptosis phenotype, we tested if overexpression of ING-3 sensitized germ cells to DNA-damage-induced apoptosis using a heat-inducible construct. No changes in the rate of germ-cell apoptosis after IR were noted (data not shown). However, we did not detect a stronger immunofluorescence signal in the germline, likely due to poor germline transgene expression (Kelly and Fire 1998).

***ing-3* results in a kinker Unc phenotype:** Applying RNAi to *ing-3* in wild type or to the RNAi-sensitive strain *rrf-3* (Simmer *et al.* 2002) resulted in no overt morphological phenotypes. The brood size of *ing-3(tm2530)* was similar to that of wild type (201 ± 62 *vs.* 220 ± 29 for N2, $n = 8$ and 7 hermaphrodites, respectively). However, both the *Mos* insertion and the *ing-3* mutants showed a weak, but fully penetrant, kinker Unc phenotype. This indicates possible neuronal function, which was likely not seen with dsRNA exposure because neurons are refractory to RNAi (Simmer *et al.* 2002).

DISCUSSION

***C. elegans ing-3* and IR-induced apoptosis:** Mammalian ING proteins have well-documented roles in apoptosis (Helbing *et al.* 1997; Garkavtsev *et al.* 1998; Shinoura *et al.* 1999; Scott *et al.* 2001; Shimada *et al.* 2002; Vieyra *et al.* 2002a; Wagner and Helbing 2005; Zhu *et al.* 2005, 2006; Feng *et al.* 2006; Wang and Li 2006; Coles *et al.* 2007). Specifically, overexpression of human *ING3*, a putative homolog of the *C. elegans ing-3* gene studied here, promotes apoptosis (Nagashima *et al.* 2003; Wang and Li 2006), and low levels of nuclear ING3 are associated with decreased survival of melanoma patients (Wang *et al.* 2007). In *C. elegans* we found that IR-induced germ-cell apoptosis was inhibited in both *ing-3(RNAi)* knockdown and *ing-3* knockouts (Figure 4, Table 1). As a result, many DNA-damaged germ cells survived and went on to form inviable zygotes (Figure 4, Table 2). Western blotting showed that RNAi reduced ING-3 levels by 50–80% (data not shown) whereas in the knockouts ING-3 was completely depleted. However, the phenotypes of the internal deletion mutant *ing-3(tm2530)* were only slightly stronger than those of the RNAi, suggesting that *C. elegans* is sensitive to relatively small changes in ING-3 levels or that the residual ING-3 after RNAi was in tissues not relevant to the phenotype.

Unlike γ-radiation, *ing-3(RNAi)* did not elevate the embryonic death rate following non-ionizing DNA-damaging treatments, including UV radiation, paraquat treatment, and heat shock (data not shown). These results suggest that, in contrast to mammalian ING proteins, *C. elegans* ING-3 may transduce signals generated by ionizing irradiation but not by other stresses. These functions may be carried out by the other two worm *ING*-related genes, and a division of labor might be expected since mammalian *ING* genes appear to function in a variety of histone acetylation complexes with potentially overlapping function (Feng *et al.* 2002; Doyon *et al.* 2006).

It is possible that the decreased number of programmed cell deaths in *ing-3* following IR resulted from the mutants simply having fewer germ cells. A number of lines of evidence argue against this possibility. First, the brood size of *ing-3(tm2180)* is similar to that of wild type. Second, if there were fewer cells that could die, then there would not have been a corresponding increase in the percentage of dead embryos following IR as we observed (Figure 4). Third, the response to IR and UV differed for *ing-3*, with only the former showing

increased embryo lethality in the mutants; alterations in germ-cell populations would affect UV and IR similarly. Fourth, if the decrease in apoptosis following IR were due to a decrease in germ-cell numbers, then the effects of *ing-3* and *cep-1* would have been additive because they were mechanistically different, which is contrary to what we found.

The roles of *ing-3* and *cep-1* in promoting stress-induced apoptosis: While dispensable for physiological germ-cell death and developmental programmed cell death (Salinas *et al.* 2006), *cep-1*, the *C. elegans* p53 homolog, is required for DNA-damage-induced apoptosis (Derry *et al.* 2001; Schumacher *et al.* 2001). In mammalian cells, ING proteins can promote p53-dependent apoptosis, but a recent report indicates that p53 and ING1 operate independently regarding sensitivity to apoptosis (Coles *et al.* 2007). In contrast to ING1 function in mammals, our data show that the IR-induced phenotypes of *ing-3*, *cep-1*, and *ing-3*; *cep-1* are very similar (Tables 1 and 2, Figure 4). This indicates that the two genes function in the same apoptotic pathway; otherwise additive effects would have been seen. Consistent with this idea, ING-3 localizes in the pachytene nuclei (Figure 3) as CEP-1 does (Schumacher *et al.* 2005). The simplest model is that the two genes act together to induce transcription of genes required for apoptosis. However, although CEP-1 induces transcription of the proapoptotic gene *egl-1* (Hofmann *et al.* 2002; Schumacher *et al.* 2005; Quevedo *et al.* 2007), preliminary evidence indicates that *ing-3(tm2830)* does not reduce the level of the *egl-1* transcript (S. Shah, unpublished results). Thus, *ing-3* may influence only a subset of *cep-1* targets, it may act downstream of CEP-1-mediated transcription, or it could function in a parallel, but nonredundant, pathway.

The function of CEP-1 and ING-3 also differs in that CEP-1 is required for both UV and IR-induced germ-cell apoptosis (Derry *et al.* 2001; Schumacher *et al.* 2001, 2005; Stergiou *et al.* 2007) while we found no role for ING-3 in the UV response. In addition to *ing-3* and *cep-1*, genes such as *abl-1*, *lin-35*, *dpl-1*, *efl-2*, *clk-2*, *hus-1*, *mrt-2*, *ced-3*, *ced-4*, and *ced-9* are also involved in DNA-damage-induced *C. elegans* germ-cell apoptosis (Deng *et al.* 2004; Schertel and Conradt 2007). How *ing-3* operates within pathways represented by these genes is unknown, although mammalian ING3 has been reported to function with the apoptotic caspase 8 in melanoma cancer cells (Wang and Li 2006).

Although we examined *ing-3* phenotypes only in the germline and embryo, ING-3, like CEP-1, is widely expressed. In addition, *ing-3* appears to be expressed differently when transcribed as part of an operon or from its own internal promoter (Figure 2). This may allow differential expression in different tissues, which in turn might reflect different functions. Both *ing-3(tm2530)* and *ing-3(ttTi5439)* mutants possess a weak kinker Unc phenotype. The kinker phenotype usually indicates a defect in neurons (Geng *et al.* 2003), a cell type in which ING-3 is expressed (Figure 2). It will be interesting to determine if ING-3 neural function is evolutionarily conserved in vertebrates (Wagner and Helbing 2005).

It is intriguing that *ing-3* resides in an operon with two other genes that could potentially influence similar processes. *hda-6* encodes a histone deacetylase while *mcd-1* encodes a C2H2 zinc-finger mediator of somatic cell death (Reddien *et al.* 2007). Although we did not detect genetic interactions between these genes and *ing-3* during germline apoptosis, they may interact with *ing-3* in other processes.

ING-3 and chromatin regulation: In both mammals and yeast, ING proteins interact with histone acetyltransferase or deacetylase complexes (reviewed in Russell *et al.* 2006). We found that ING-3 overlapped the DAPI pattern throughout the cell cycle, suggesting that ING-3 might function in chromatin regulation as suggested by reports showing a direct interaction between the PHD regions of mammalian ING proteins and histone H3 (Martin *et al.* 2006; Pena *et al.* 2006; Shi *et al.* 2006). The staining of ING-3 was not evenly distributed on chromatin, suggesting that ING-3 might accumulate in specific regions. If so, ING-3 might regulate chromatin structure with associated HAT and HDAC complexes and influence gene silencing or transcription in *C. elegans* as previously reported in cell culture systems.

We thank members of the Riabowol and Mains labs and members of the Calgary *C. elegans* group, in particular J. Gaudet, J. D. McGhee, and D. Hansen, as well as the anonymous reviewers, for discussion and help with methods. We thank S. Mitani and L. Segalat for generously providing *ing-3* mutants and the *Caenorhabditis* Genetics Center (funded by the National Institutes of Health, Center for Research Resources) for providing strains. We thank the Southern Alberta Cancer Research Institute Hybridoma Facility for generating antibodies and Susan Lees-Miller for providing the ionizing irradiation source. This work was supported by grants from the Canadian Institutes of Health Research (CIHR) and the Alberta Cancer Board to K.R. and grants from the CIHR and the Alberta Heritage Foundation for Medical Research to P.E.M.

LITERATURE CITED

Bienz, M., 2006 The PHD finger, a nuclear protein-interaction domain. Trends Biochem. Sci. **31:** 35–40.

Blumenthal, T., and K. Steward, 1997 RNA processing and gene structure, pp. 117–146 in *C. elegans II*, edited by D. L. Riddle, T. Blumenthal, B. J. Meyer and J. R. Priess. Cold Spring Harbor Laboratory Press, Cold Spring Harbor, NY.

Brenner, S., 1974 The genetics of *Caenorhabditis elegans*. Genetics **77:** 71–94.

Cheung, K. J., Jr, J. A. Bush, W. Jia, and G. Li, 2000 Expression of the novel tumour suppressor p33(ING1) is independent of p53. Br. J. Cancer **83:** 1468–1472.

Clark, S. G., X. Lu and H. R. Horvitz, 1994 The *Caenorhabditis elegans* locus *lin-15*, a negative regulator of a tyrosine kinase signaling pathway, encodes two different proteins. Genetics **137:** 987–997.

Coles, A. H., H. Liang, Z. Zhu, C. G. Marfella, J. Kang *et al.*, 2007 Deletion of p37Ing1 in mice reveals a p53-independent

role for Ing1 in the suppression of cell proliferation, apoptosis, and tumorigenesis. Cancer Res. **67:** 2054–2061.

Deng, X., E. R. Hofmann, A. Villanueva, O. Hobert, P. Capodieci *et al.*, 2004 *Caenorhabditis elegans* ABL-1 antagonizes p53-mediated germline apoptosis after ionizing irradiation. Nat. Genet. **36:** 906–912.

Derry, W. B., A. P. Putzke and J. H. Rothman, 2001 *Caenorhabditis elegans* p53: role in apoptosis, meiosis, and stress resistance. Science **294:** 591–595.

Doyon, Y., C. Cayrou, M. Ullah, A. J. Landry, V. Cote *et al.*, 2006 ING tumor suppressor proteins are critical regulators of chromatin acetylation required for genome expression and perpetuation. Mol. Cell **21:** 51–64.

Feng, X., Y. Hara and K. Riabowol, 2002 Different HATS of the ING1 gene family. Trends Cell Biol. **12:** 532–538.

Feng, X., S. Bonni and K. Riabowol, 2006 HSP70 induction by ING proteins sensitizes cells to tumor necrosis factor alpha receptor-mediated apoptosis. Mol. Cell. Biol. **26:** 9244–9255.

Garkavtsev, I., A. Kazarov, A. Gudkov and K. Riabowol, 1996 Suppression of the novel growth inhibitor p33ING1 promotes neoplastic transformation. Nat. Genet. **14:** 415–420.

Garkavtsev, I., I. A. Grigorian, V. S. Ossovskaya, M. V. Chernov, P. M. Chumakov *et al.*, 1998 The candidate tumour suppressor p33ING1 cooperates with p53 in cell growth control. Nature **391:** 295–298.

Gartner, A., S. Milstein, S. Ahmed, J. Hodgkin and M. O. Hengartner, 2000 A conserved checkpoint pathway mediates DNA damage-induced apoptosis and cell cycle arrest in *C. elegans*. Mol. Cell **5:** 435–443.

Gartner, A., A. J. MacQueen and A. M. Villeneuve, 2004 Methods for analyzing checkpoint responses in *Caenorhabditis elegans*. Methods Mol. Biol. **280:** 257–274.

Geng, W., P. Cosman, J. H. Baek, C. C. Berry and W. R. Schafer, 2003 Quantitative classification and natural clustering of *Caenorhabditis elegans* behavioral phenotypes. Genetics **165:** 1117–1126.

Gengyo-Ando, K., and S. Mitani, 2000 Characterization of mutations induced by ethyl methanesulfonate, UV, and trimethylpsoralen in the nematode *Caenorhabditis elegans*. Biochem. Biophys. Res. Commun. **269:** 64–69.

Gozani, O., P. Karuman, D. R. Jones, D. Ivanov, J. Cha *et al.*, 2003 The PHD finger of the chromatin-associated protein ING2 functions as a nuclear phosphoinositide receptor. Cell **114:** 99–111.

Granger, L., E. Martin and L. Segalat, 2004 *Mos* as a tool for genome-wide insertional mutagenesis in *Caenorhabditis elegans*: results of a pilot study. Nucleic Acids Res. **32:** e117.

Gumienny, T. L., E. Lambie, E. Hartwieg, H. R. Horvitz and M. O. Hengartner, 1999 Genetic control of programmed cell death in the *Caenorhabditis elegans* hermaphrodite germline. Development **126:** 1011–1022.

Han, X., X. Feng, J. B. Rattner, H. Smith, P. Bose *et al.*, 2008 Tethering by lamin A stabilizes and targets the ING1 tumour suppressor. Nat. Cell Biol. **10:** 1333–1340.

Hansen, D., L. Wilson-Berry, T. Dang and T. Schedl, 2004 Control of the proliferation versus meiotic development decision in the *C. elegans* germline through regulation of GLD-1 protein accumulation. Development **131:** 93–104.

He, G. H., C. C. Helbing, M. J. Wagner, C. W. Sensen and K. Riabowol, 2005 Phylogenetic analysis of the ING family of PHD finger proteins. Mol. Biol. Evol. **22:** 104–116.

Helbing, C. C., C. Veillette, K. Riabowol, R. N. Johnston and I. Garkavtsev, 1997 A novel candidate tumor suppressor, ING1, is involved in the regulation of apoptosis. Cancer Res. **57:** 1255–1258.

Hofmann, E. R., S. Milstein, S. J. Boulton, M. Ye, J. J. Hofmann *et al.*, 2002 *Caenorhabditis elegans* HUS-1 is a DNA damage checkpoint protein required for genome stability and EGL-1-mediated apoptosis. Curr. Biol. **12:** 1908–1918.

Huang, L. S., P. Tzou and P. W. Sternberg, 1994 The *lin-15* locus encodes two negative regulators of *Caenorhabditis elegans* vulval development. Mol. Biol. Cell **5:** 395–411.

Kaadige, M. R., and D. E. Ayer, 2006 The polybasic region that follows the plant homeodomain zinc finger 1 of Pf1 is necessary and sufficient for specific phosphoinositide binding. J. Biol. Chem. **281:** 28831–28836.

Kelly, W. G., and A. Fire, 1998 Chromatin silencing and the maintenance of a functional germline in *Caenorhabditis elegans*. Development **125:** 2451–2456.

Kichina, J. V., M. Zeremski, L. Aris, K. V. Gurova, E. Walker *et al.*, 2006 Targeted disruption of the mouse ing1 locus results in reduced body size, hypersensitivity to radiation and elevated incidence of lymphomas. Oncogene **25:** 857–866.

Lettre, G., E. A. Kritikou, M. Jaeggi, A. Calixto, A. G. Fraser *et al.*, 2004 Genome-wide RNAi identifies p53-dependent and -independent regulators of germ cell apoptosis in *C. elegans*. Cell Death Differ. **11:** 1198–1203.

Loewith, R., M. Meijer, S. P. Lees-Miller, K. Riabowol and D. Young, 2000 Three yeast proteins related to the human candidate tumor suppressor p33(ING1) are associated with histone acetyltransferase activities. Mol. Cell. Biol. **20:** 3807–3816.

Martin, D. G., K. Baetz, X. Shi, K. L. Walter, V. E. Macdonald *et al.*, 2006 The Yng1p plant homeodomain finger is a methyl-histone binding module that recognizes lysine 4-methylated histone H3. Mol. Cell. Biol. **26:** 7871–7879.

Mello, C. C., J. M. Kramer, D. Stinchcomb and V. Ambros, 1991 Efficient gene transfer in *C. elegans*: extrachromosomal maintenance and integration of transforming sequences. EMBO J. **10:** 3959–3970.

Miller, D. M., and D. C. Shakes, 1995 Immunofluorescence microscopy, pp. 365–394 in *Caenorhabditis elegans: Modern Biological Analysis of an Organism*, edited by H. F. Epstein and D. C. Shakes. Academic Press, San Diego.

Nagashima, M., M. Shiseki, K. Miura, K. Hagiwara, S. P. Linke *et al.*, 2001 DNA damage-inducible gene p33ING2 negatively regulates cell proliferation through acetylation of p53. Proc. Natl. Acad. Sci. USA **98:** 9671–9676.

Nagashima, M., M. Shiseki, R. M. Pedeux, S. Okamura, M. Kitahama-Shiseki *et al.*, 2003 A novel PHD-finger motif protein, p47ING3, modulates p53-mediated transcription, cell cycle control, and apoptosis. Oncogene **22:** 343–350.

Nourani, A., L. Howe, M. G. Pray-Grant, J. L. Workman, P. A. Grant *et al.*, 2003 Opposite role of yeast ING family members in p53-dependent transcriptional activation. J. Biol. Chem. **278:** 19171–19175.

Palacios, A., P. Garcia, D. Padro, E. Lopez-Hernandez, I. Martin *et al.*, 2006 Solution structure and NMR characterization of the binding to methylated histone tails of the plant homeodomain finger of the tumour suppressor ING4. FEBS Lett. **580:** 6903–6908.

Pena, P. V., F. Davrazou, X. Shi, K. L. Walter, V. V. Verkhusha *et al.*, 2006 Molecular mechanism of histone H3K4me3 recognition by plant homeodomain of ING2. Nature **442:** 100–103.

Quevedo, C., D. R. Kaplan and W. B. Derry, 2007 AKT-1 regulates DNA-damage-induced germline apoptosis in *C. elegans*. Curr. Biol. **17:** 286–292.

Reddien, P. W., E. C. Andersen, M. C. Huang and H. R. Horvitz, 2007 DPL-1 DP, LIN-35 Rb and EFL-1 E2F act with the MCD-1 zinc-finger protein to promote programmed cell death in *Caenorhabditis elegans*. Genetics **175:** 1719–1733.

Russell, M., P. Berardi, W. Gong and K. Riabowol, 2006 Grow-ING, Age-ING and Die-ING: ING proteins link cancer, senescence and apoptosis. Exp. Cell Res. **312:** 951–961.

Salinas, L. S., E. Maldonado and R. E. Navarro, 2006 Stress-induced germ cell apoptosis by a p53 independent pathway in *Caenorhabditis elegans*. Cell Death Differ. **13:** 2129–2139.

Schertel, C., and B. Conradt, 2007 *C. elegans* orthologs of components of the RB tumor suppressor complex have distinct pro-apoptotic functions. Development **134:** 3691–3701.

Schumacher, B., K. Hofmann, S. Boulton and A. Gartner, 2001 The *C. elegans* homolog of the p53 tumor suppressor is required for DNA damage-induced apoptosis. Curr. Biol. **11:** 1722–1727.

Schumacher, B., C. Schertel, N. Wittenburg, S. Tuck, S. Mitani *et al.*, 2005 *C. elegans ced-13* can promote apoptosis and is induced in response to DNA damage. Cell Death Differ. **12:** 153–161.

Scott, M., P. Bonnefin, D. Vieyra, F. M. Boisvert, D. Young *et al.*, 2001 UV-induced binding of ING1 to PCNA regulates the induction of apoptosis. J. Cell Sci. **114:** 3455–3462.

Shaham, S. (Editor), 2006 *WormBook: Methods in Cell Biology*, edited by The *C. elegans* Research Community. *WormBook*, http://www.wormbook.org.

Shi, X., T. Hong, K. L. Walter, M. Ewalt, E. Michishita *et al.*, 2006 ING2 PHD domain links histone H3 lysine 4 methylation to active gene repression. Nature **442:** 96–99.

Shimada, H., T. L. Liu, T. Ochiai, T. Shimizu, Y. Haupt *et al.*, 2002 Facilitation of adenoviral wild-type p53-induced apoptotic cell death by overexpression of p33(ING1) in T.Tn human esophageal carcinoma cells. Oncogene **21:** 1208–1216.

Shinoura, N., Y. Muramatsu, M. Nishimura, Y. Yoshida, A. Saito *et al.*, 1999 Adenovirus-mediated transfer of p33ING1 with p53 drastically augments apoptosis in gliomas. Cancer Res. **59:** 5521–5528.

Shiseki, M., M. Nagashima, R. M. Pedeux, M. Kitahama-Shiseki, K. Miura *et al.*, 2003 p29ING4 and p28ING5 bind to p53 and p300, and enhance p53 activity. Cancer Res. **63:** 2373–2378.

Simmer, F., M. Tijsterman, S. Parrish, S. P. Koushika, M. L. Nonet *et al.*, 2002 Loss of the putative RNA-directed RNA polymerase RRF-3 makes *C. elegans* hypersensitive to RNAi. Curr. Biol. **12:** 1317–1319.

Soliman, M. A., and K. Riabowol, 2007 After a decade of study-ING, a PHD for a versatile family of proteins. Trends Biochem. Sci. **32:** 509–519.

Stergiou, L., K. Doukoumetzidis, A. Sendoel and M. O. Hengartner, 2007 The nucleotide excision repair pathway is required for UV-C-induced apoptosis in *Caenorhabditis elegans*. Cell Death Differ. **14:** 1129–1138.

Takanami, T., A. Mori, H. Takahashi and A. Higashitani, 2000 Hyper-resistance of meiotic cells to radiation due to a strong expression of a single recA-like gene in *Caenorhabditis elegans*. Nucleic Acids Res. **28:** 4232–4236.

Timmons, L., D. L. Court and A. Fire, 2001 Ingestion of bacterially expressed dsRNAs can produce specific and potent genetic interference in *Caenorhabditis elegans*. Gene **263:** 103–112.

Treinin, M., B. Gillo, L. Liebman and M. Chalfie, 1998 Two functionally dependent acetylcholine subunits are encoded in a single *Caenorhabditis elegans* operon. Proc. Natl. Acad. Sci. USA **95:** 15492–15495.

Vieyra, D., T. Toyama, Y. Hara, D. Boland, R. Johnston *et al.*, 2002a ING1 isoforms differentially affect apoptosis in a cell age-dependent manner. Cancer Res. **62:** 4445–4452.

Vieyra, D., R. Loewith, M. Scott, P. Bonnefin, F. M. Boisvert *et al.*, 2002b Human ING1 proteins differentially regulate histone acetylation. J. Biol. Chem. **277:** 29832–29839.

Wagner, M. J., and C. C. Helbing, 2005 Multiple variants of the ING1 and ING2 tumor suppressors are differentially expressed and thyroid hormone-responsive in Xenopus laevis. Gen. Comp. Endocrinol. **144:** 38–50.

Wang, Y., and G. Li, 2006 ING3 promotes UV-induced apoptosis via Fas/caspase-8 pathway in melanoma cells. J. Biol. Chem. **281:** 11887–11893.

Wang, Y., D. L. Dai, M. Martinka and G. Li, 2007 Prognostic significance of nuclear ING3 expression in human cutaneous melanoma. Clin. Cancer Res. **13:** 4111–4116.

Zdinak, L. A., I. B. Greenberg, N. J. Szewczyk, S. J. Barmada, M. Cardamone-Rayner *et al.*, 1997 Transgene-coded chimeric proteins as reporters of intracellular proteolysis: starvation-induced catabolism of a LacZ fusion protein in muscle cells of *Caenorhabditis elegans*. J. Cell Biochem. **67:** 143–153.

Zhu, J. J., F. B. Li, X. F. Zhu and W. M. Liao, 2006 The p33ING1b tumor suppressor cooperates with p53 to induce apoptosis in response to etoposide in human osteosarcoma cells. Life Sci. **78:** 1469–1477.

Zhu, Z., J. Lin, J. H. Qu, M. A. Feitelson, C. R. Ni *et al.*, 2005 Inhibitory effect of tumor suppressor p33(ING1b) and its synergy with p53 gene in hepatocellular carcinoma. World J. Gastroenterol. **11:** 1903–1909.

Communicating editor: D. I. Greenstein